Heliyon 10 (2024) e28380

Contents lists available at ScienceDirect

Heliyon

journal homepage: www.cell.com/heliyon

Research article

Performance and CO_2 emission of a single cylinder compression ignition engine powered by *Khaya senegalensis* non-edible seeds fuel blends

Elijah Eferoghene Onojowho [a,e,*], Eriola Betiku [b,c], Abraham Awolola Asere [a,d]

[a] Department of Mechanical Engineering, Obafemi Awolowo University, Ile-Ife, Nigeria
[b] Department of Chemical Engineering, Obafemi Awolowo University, Ile-Ife, Nigeria
[c] Department of Biology, Florida Agricultural and Mechanical University, Tallahassee, FL 32307, USA
[d] Department of Automobile Engineering, Elizade University Ilara-Mokin, Nigeria
[e] Department of Mechanical Engineering, University of Nigeria, Nsukka, Nigeria

ARTICLE INFO

Keywords:
ICE
Khaya senegalensis fuel combustion
Numerical-experimental engine performance comparison
Binary blending properties
Carbon (iv) oxide emission

ABSTRACT

This work aimed at investigating blends of *Khaya senegalensis* biodiesel in a compression ignition engine, attempting to improve engine performance and reduce CO_2 emission compared with conventional diesel. Analysis of System (ANSYS) was used to predict in-cylinder behavior of the fuel. ANSYS SpaceClaim generated the geometric model on which 5° sector and mesh refinement was on ANSYS Internal Combustion Engine Modeler (ICEM). Computational domain of interest lies within the compression and expansion strokes. Experimental validation followed: 5% biodiesel, 95% diesel (B_5); 15% biodiesel, 85% diesel (B_{15}); 25% biodiesel, 75% diesel (B_{25}); pure diesel (D_{100}); pure biodiesel (B_{100}) in volume proportions. B_{15} has the highest brake mean effective pressure (BMEP) of 4 bar as load increases. An experimental and numerical comparison reveals pressure declination against speed increment. Ignition temperature fluctuated between 799.76 and 806.256 K for D_{100} and 760.73–790.62 K for B_{100} within 1800–2800 rpm speed limit prediction. Power and brake thermal efficiency (BTE) had parallel load increment with all blends. CO_2 emission on increasing load conditions were 47.01%, 8.07%, 21.72% and 6.06% for B_5, B_{15}, B_{25}, and B_{100} respectively lower than D_{100}. Pressure and temperature contours gave proper combustion predicted behaviors. All blends possess replaceable performance potential for D_{100} however, B_5 offers better reliable potentials.

1. Introduction

Performance and emissions have necessitated ongoing surrogate fuel research for conventional diesel. Surrogate fuel such as hydrogen, ammonia, methanol and biofuel are common considerations for conventional fuel with ICE. However, biodiesel among others has been characterized with adequate lubricity, high miscibility with conventional fuels, low toxicity, low oxidative and corrosive properties as advantages [1]. There have been four major determining stakeholders of biofuel that should be satisfied: engine manufacturers, users or consumer, environment and socio-economy [2]. In this regard, the usage of biodiesel in engine is influenced by three major factors [3]. They are: eco-safety impact factor which is combustion emission based; engine factor, a pointer to engine

* Corresponding author. P. O. Box 41, Abraka, Nigeria.
E-mail address: efe.elijah@gmail.com (E.E. Onojowho).

https://doi.org/10.1016/j.heliyon.2024.e28380
Received 22 November 2022; Received in revised form 4 March 2024; Accepted 18 March 2024
Available online 24 March 2024

elements and combustion performance; fuel characteristic factor, satisfying mobility or flow [4]. Some identified barriers in literature rocking the application of biofuel across the globe are: feedstock availability, maturity duration and food vs fuel competition [2,5]; unstable policies, emission reduction mandate [6–9]; fossil fuel subsidies, biofuel production cost and price [10,11]; social impact uncertainties, consumer's/user's confidence [12,13]; vehicle technological variation through blend wall and engine compatibility [14,15]. The European Academies Science Advisory Council on biodiesel studies classified it into four generations on feedstock bases as first (edible feedstock), second (non-edible feedstock), third (waste feedstock) and fourth (solar assisted feedstock) generations. Zhang et al. [16] projected ternary biodiesel blend in addition to advance after-treatment as potential study trend. BNEF [17] made a prospect treat survey of electric vehicle on biofuel and said light-duty vehicle has the potentials of existing in the market till 2050s even at the taking-off of electric vehicle. In addition, estimate of 25% CO_2 reduction by 2050 from the utility of biodiesel has been projected [18], hence the need for better performance and lower emission research are needed. Beyond the in-land engine crushing, biofuel is gaining much applicative expression in marine engine presenting three main potential production routes for hydrogen, ammonia and methanol green fuels. These major routes are seawater electrolysis, applying green power; combination of hydrogen and Haber-Bosch process; and green power application in methanolysis for hydrogen, ammonia and methanol green fuels production respectively [19].

Optimization study on combustion and emission of ternary fuel blends with concentration on pre-injection timing and fuel ratio variables in marine engine reveal that early pre-injection fuel timing and higher pre-injection fuel mass ratio will translate into lesser hydrocarbon and carbon (II) oxide emissions [20]. A future prospect prediction of the Indian contribution on combustion emission seeks to redress issues stemming from the energy sources and economic perspectives in an optimal study using various optimization algorithms [21]. On marine diesel engine, Tan et al. [22] conducted a response surface methodology performance optimization of hydrogen, biodiesel and water additive on fuel blends performance. They said blending hydrogen and water to combusted fuel made significant effect at 99% confidence level to improving BSFC, BTE and reducing hydrocarbon and carbon (II) oxide emissions in the multi-objective optimization study. The effect of additives like nanoplatelets has been investigated on engine performance and emission [23–26]. In these studies, surfactant is to improve fuel stability including nanofuels. Nanoparticles have been noted with high soot accumulation, engine element wears and corrosion, low engine performance and fuel instability limitations [27], however, Zhang et al. [28] reported low hydrocarbon emission with biodiesel fuel courtesy of catalyst additive. In addition, sodium dodecyl sulphate additive on nanofuel achieved fuel blends stability [29].

Work has been done in the prediction of ICE performance using different numerical computational tools with biodiesel. Barot et al. [30] presented a flow rate study of fuel at induction stroke from injector system into chamber while Aghbashlo et al. [31] summarized machine learning application in engine combustion and performance parameters determination. A HCCI ICE simulation on KIVA3VR2-CHEMKIN software with butanol-heptane-air mixture gearing towards performance optimization to determine pollution formation and ignition delay reduction was studied [32]. Furthermore, Zhang et al. [33] investigated on AVL-Fire and CHEMKIN numerical tools and accompanied their study with experimental validation on performance, combustion and emission of ternary fuel with extensive uncertainty analysis of experimented quantities. The ternary fuel which involved ethanol, n-butanol and diesel increased BSFC, cylinder pressure and temperature, brake power and BTE on blending proportions and engine loading variation as reported. On ANSYS fluent, researchers [34,35] submitted their computational fluid dynamics findings of biodiesel and diesel combustion on velocity magnitude, temperature and pressure parameters claiming a good similarity between the experimental and numerical results.

Following further works on performance and emission from ICE experimentations, much has been done and few highlights are presented. Direct injection diesel engine combustion from rapeseed, soybean and sandbox biodiesel as independently studied at 5%, 10%, 20%, 30%, 50%, and 70% with conventional diesel has been reported in literature with keen attention on performance parameters like BSFC, engine power, BTE and CO, CO_2, NO_x, unburnt hydrocarbon emissions [36–38]. A progressive study went into equal oil proportion combination from mahua and simarouba seeds biodiesel to determine its performance, soot deposit, emissions and metal wears with reference to petrodiesel [39,40]. A hybrid combustion of CAI with SI studied by Yang and Zhao [41,42], visualized combustion process in the investigation of injection timing and park discharge effect on heat release rate and the combustion earlier stage. Semin et al. [43] made steady-state and transient CFD and experimental validation study on in-cylinder pressure in a compressed natural gas engine. In addition, pure palm biodiesel, in an experiment, was ran on a small farm powering diesel engine over 800 h duration. The ferrographic result shows that if the oil is stable, the biodiesel will make a good diesel surrogate with efficient reliability, better durability and low metal wear rate effect [44]. An electric dynamometer fitted to a small diesel engine test bed was developed by

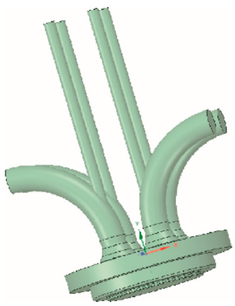

Fig. 1. Modelled engine geometry.

Grobbelaar [45] exploiting its ability to instrument diesel engine performance at various conditions with a developed software.

The non-edible feedstock *Khaya senegalensis* seed otherwise called African mahogany from Nigeria has medical, agricultural, engineering and traditional value. In literature, biodiesel production from this seed is presented, however, no numerical and experimental data exist about its performance in an ICE. Hence, the originality of this work sufficiently contributed to the knowledge base of biodiesel with the following objectives: numerically study combustion performance and CO_2 emission of the produced *Khaya senegalensis* biodiesel blends in an ICE; experimentally validating the prediction accuracy at the same condition comparable. The performance characterization was between a torque limit of 1.5 Nm and 5.5 Nm of the engine capacity.

2. Materials and methods

Engine 3D geometry modelling was done with ANSYS SpaceClaim (SCDM 17.2) as shown in Fig. 1 with four straight valves and bowl-shaped piston which was decomposed at IVC into different zones, layers and an end-product 5° sectored geometry by ANSYS design modeler. This was fine meshed into elements and nodes under ICEM. Dynamic mesh control was applied at grid independence development of zones. Boundary layer conditions for the zones were basically wall and fluid created of temperature and pressure variables. Engine, fuel and air materials were ANSYS fluent based and in combination with Onojowho et al. [46] determined material. The compression and expansion strokes were the simulation scope using ANSYS Fluent v19. R3 on Hewlett-Packard Desktop workstation setup of Table 1 and the summary of simulation details is as presented in Table 2.

Experimented blends of fuel were poured into the TecQuipment Ltd engine test rig fitted with hydraulic dynamometer to make load variations shown in Fig. 2. Gas analyzer in Table 3 was used to capture the emissions of the combustion while engine performance with various blends were reported on desktop.

The uncertainties analysis of experimental data errors in this study was determined using the square root of the sum of the squares approach [47]. The analysis is made up of mean values of repeated measurements which estimated the actual value for individual parameters of various measuring equipment. Error sources were mainly random and systemic in nature. Percentage uncertainties of measurand are illustrated in Table 4.

3. Theory/calculation

This internal combustion engine simulation phenomenon involved numerous complex models. Few fundamentals are mentioned. Energy model that employs the turbulent viscous flow, the RNG k-ε Eqs. (1) and (2) are chosen with near wall treatment of the viscous flow. Transport species model of Eq. (3) did handle the combustion chemistry interaction activities. Auto-ignition of the direct ignition combustion process was expressed by the Hardenburg model of Eq. (4). Discrete phase models of particle behaviors are Eqs. (5) and (6) for particle collision model and Kuhnke model of boundary layer behavior respectively. The decomposition of wall boundary layer domain into zones was accounted for with Eq. (6b) while flow regimes and droplet properties were expressed with Eq. (6a). Fundamental combustion Eq. (7) is always applied for reaction equilibrium. All equations are ANSYS Fluent embedded.

On experimental base, Eqs. (8)–(10) were inbuilt in TecQuipment Ltd software to determine engine power developed, BTE and BMEP. In this work, statistical assessment of uncertainty analysis combines all errors using Eq. (11) for the estimate.

$$\partial(\rho k)/\partial t+\partial(\rho k u_i)/\partial x_i=\partial\left[\left(\mu+\rho C_\mu k^2/\varepsilon/\sigma_k\right)\partial k/\partial x_j\right]/\partial x_j+G_k-\rho\varepsilon+S_{near-wall} \tag{1}$$

$$\partial(\rho\varepsilon)/\partial t+\partial(\rho\varepsilon u_i)/\partial x_i=\partial\left[\left\{\mu+\left(\rho C_\mu k^2/\varepsilon\right)/\sigma_\varepsilon\right\}\partial k/\partial x_j\right]/\partial x_j+C_{1\varepsilon}\varepsilon/KG_k-C_{2\varepsilon}\rho\varepsilon^2/K \tag{2}$$

$$\partial(\rho Y_i)\Big/\partial t+\nabla\cdot(\rho\vec{v}Y_i)=-\nabla\cdot\vec{J_I}+R_i+S_i \tag{3}$$

$$\partial\rho Y_{ig}\Big/\partial t+\nabla\cdot\left(\rho\vec{v}Y_{ig}\right)=\nabla\cdot\left(\mu_t/Sc_t\nabla Y_{ig}\right)+\rho\int_{t=t_o}^{t}dt\Big/\tau_{ig} \tag{4}$$

$$We_c=\rho u_{rel}^2\overline{D}/\sigma \tag{5}$$

Table 1
Simulation system specification.

Items		Specification
1.	System type	64-bit OS, x64-based processor
2.	System model	HP Z820 workstation
3.	Operating system and version	Windows 10 Pro and 10.0.17,763 build 17,763
4.	Booting device	\Device\Harddiskvolume2
5.	Processor	Intel (R) Xeon (R) CPU E5-2670 0 @ 2.60 GHz, 2601 MHz (and 2594 MHz), 8 core(s), 16 Logical Processor(s).
6.	Installed RAM	128 GB and 120 GB (Physical Memory)
7.	BIOS device and mode	Hewlett-Packard J63 v03.94 and UEFI

Table 2
Summary of simulation parameters.

Parameters		Values
1.	Inlet valve close (IVC)	225 CA (45° ABDC)
2.	Exhaust valve opening (EVC)	500 CA (40° BBDC)
3.	Compression ratio	22:1
4.	Bore and Stroke	69 and 62 mm
5.	Engine speed	1800, 2300, 2800 rpm
6.	Number of cylinders	single
7.	Connecting rod length and crank radius	104 and 43.28 mm
8.	Min., Max. valve lift and piston offset	0.2, 2 mm and 0°
9.	Injection spray angle	6°
10.	Mesh elements and nodes	123,253 and 162,828
11.	Max. and min. mesh size	0.321 and 0.129 mm
12.	Mesh reference size	0.642 mm
13.	Chamber body mesh size	1.993 mm
14.	Number of inflation layer	5
15.	Crevice H/T ratio	3

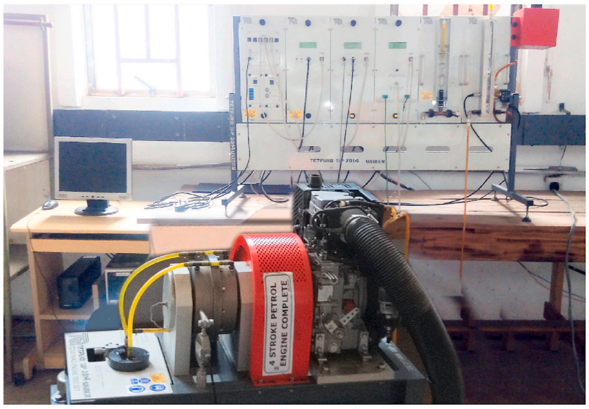

Fig. 2. Single cylinder engine test rig setup.

Table 3
Engine test rig specification.

Parameters		Values
1.	Dynamometer const. head	1 bar @ 5 L/min (min.)
2.	Dynamometer max. power and speed rating	7.5 KW and 7000 rpm
3.	Engine cylinder, capacity and stroke	Single, 0.232 L and 4
4.	Engine max. rating	3.5 KW @ 3600 rpm
5.	Bore, stroke and crank radius	69/62/31 mm
6.	Connecting rod length	104 mm
7.	Compression ratio	22:1
8.	Thermocouple	Type-k
9.	Gas analyzer model	Testo 330-2LL
10.	Engine model	TD212, TQ182785-002
11.	Brand	TecQuipment Ltd

Table 4
Experiment measurands accuracies and their uncertainties.

Parameters		Range	Accuracy	Uncertainty
1.	BMEP	–	–	±0.0823 bar
2.	BTE	–	–	±1.29 %
3.	Power	–	±3 %	±21.98 W
4.	Temperature	0–1000 °C	3%	±0.5 °C
5.	CO_2	0–1,000,000 ppm	+3 %	±0.22 %

$$K = \left(\rho u^2 d_p / \sigma\right)^{5/8} \left(\sigma \rho d_p / \mu^2\right)^{1/8} \tag{6a}$$

$$T^* = T_w / T_{sat} \tag{6b}$$

$$C_n H_m O_c + (n + m/4)(O_2 + 3.74 N_2) \rightarrow nCO_2 + m/2 H_2O + (n + m/4) 3.76 N_2 \tag{7}$$

$$P = 2\pi N(rpm)\tau(Nm)/60 \tag{8}$$

$$BTE = P / H_f \times 100 \tag{9}$$

$$BMEP(bar) = 60Ps/2/0.1N(rpm)e_c(cc) \tag{10}$$

$$U_r = \sqrt{\sum_{i=1}^{1} \left(U_{\overline{X}_i} \partial r / \partial x_{i_{x=\overline{x}}}\right)^2} \tag{11}$$

$$U_r = \sqrt{BMEP^2 + BTE^2 + P^2 + Temperature^2 + CO_2{}^2} = \pm 22.02 \tag{12}$$

Where G_k is a turbulence kinetic mean velocity gradient, $S_{near\text{-}wall}$ is a near-wall viscous source factor, $C_{1\varepsilon}$, $C_{2\varepsilon}$, C_μ, σ_k, and σ_ε are model constants, Y_i, S_i and R_i are local mass fraction, total rate of dispersed phase and source, net rate production for ith species. Ignition delay factor is τ_{ig}, mass fraction of atomized species Y_{ig}, fuel enter time t_o, diffusion time t, Schmidt number Sc_t, Weber number We_c, mean diameter $\overline{D}$, ρ and σ are density and surface tension, mechanical developed power P, engine torque τ, fuel heat released H_f, stroke s, kinetic and dissipation energies k-ε, speed N and engine capacity e_c. In Eq. (11), a measured value is r, $U_{\overline{X}_i}$ is related to a measurand, at $i = 1,2, \ldots, l$. The sensitivity index of the measuring device or equipment for a repeatability process is expressed with $\partial r / \partial x_{i_{x=\overline{x}}}$ while U_r is the overall result uncertainty.

4. Results and discussion

4.1. Power developed

Brake power developed from experimentation in Fig. 3 makes a direct increase relationship with engine speed, hence engine torque increases. All blends yielded as expected, however, B_{15} tends to be more reliable in same trend with literature [48,49].

4.2. BMEP

Numerically, Fig. 4 predicted significant pressure rise to begin from the fuel injection period of the compression stroke to ignition periods while peak pressure was at combustion period for all blend irrespective of engine speeds. In-cylinder combustion peak pressures will drop steadily from 6.3358 to 6.1438 exp6 Pa on speed increment within 340°–359° CA combustion period from the prediction. The pressure contour plot at 1800 rpm and 357° CA for D_{100} and B_{100} are given in Figs. 5 and 6 indicating more combustion requirement for D_{100}.

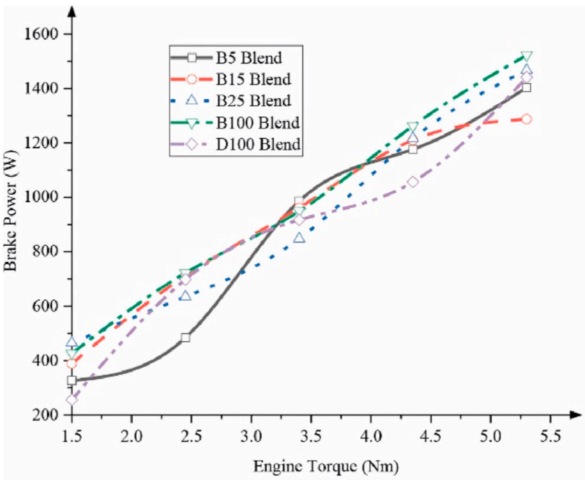

Fig. 3. Brake power performance of experimented blends.

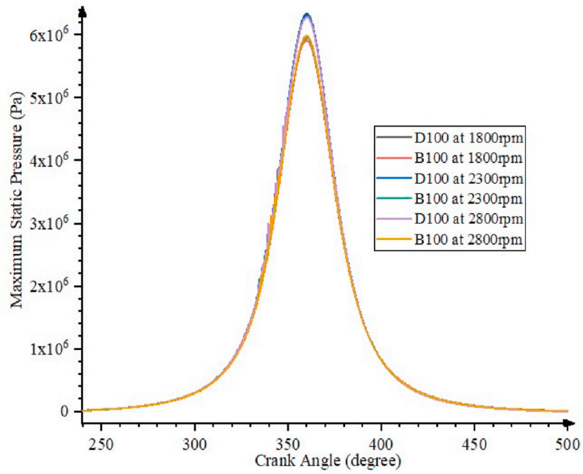

Fig. 4. CFD combustion in-cylinder pressure plots.

Experimentally, BMEP decreases with a corresponding rise in engine speed to validate the numerical prediction. This holds true from the torque-speed inverse relationship in BMEP relation. Hence, Fig. 7 presents B_{15} as the highest BMEP as load increases.

4.2.1. Numerical-experimental contrast of B_{100} and D_{100} performance

In Fig. 8, B_{100} combustion in-cylinder pressure and temperature are confirmed to be greater than D_{100} due to the higher LHV of B_{100} as presented in Table 5 which is a highlight of physicochemical properties characterization of produced fuel blends [46] and it conforms with existing work [50]. Similarly, an increase in engine speed translated into an in-cylinder combustion pressure decrease as numerically predicted and experimentally validated.

4.3. Combustion temperature

Numerical plot of Fig. 9 reveals that for D_{100}, ignition temperature will exist between 799.76 K and 806.26 K at 339°–339.55° CA and combustion period will be 340°–360° CA at all speed. Peak combustion temperature of 973.66 K (at 359.25° CA), 973.96 K (at 359° CA) and 976.73 K (at 357° CA) will be obtained in the order of 1800 rpm, 2300 rpm and 2800 rpm respectively. With B_{100}, there will a longer combustion period between 338° and 376° CA for the speeds. This suggests a complete combustion of mixture and that B_{100} contains more volatile matter. Rapid ignition occurred more in B_{100} within 760.73 K–790.62 K at 336.3°–342° CA while combustion peak temperature of 931.41 K, 934.36 K and 935.49 K in a uniform 359.5° CA will exist in the same order of speed.

Temperature contours of Figs. 10 and 11 strengthen the D_{100} higher combustion temperature submission of the plot in Fig. 9. They are contours of combustion at TDC reflecting flame progression around piston surface zone at 349° CA of 2300 rpm. Both contours predict flame base to exist at the piston surface while zones of peak temperature are wall boundary zones. Expansion stroke period for B_{100} is shorter by 19° CA difference at 2800 rpm. In-cylinder expansion temperature of Figs. 12 and 13 are observed to be cooler as piston moves closer to BDC for D_{100} and B_{100} respectively at 2800 rpm. These depict chambers non combustion zones.

4.4. Engine efficiency: BTE

BTE as a function of brake power and heat of combustion describes the ability of the engine to convert chemical energy into useful

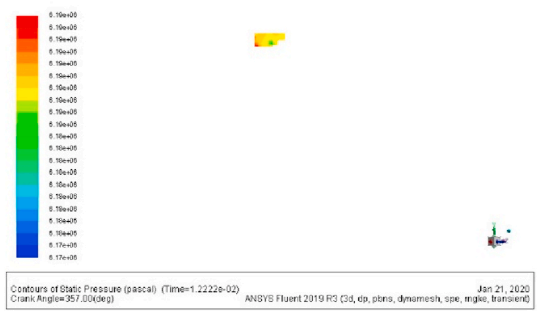

Fig. 5. D_{100} in-cylinder CFD combustion pressure contour.

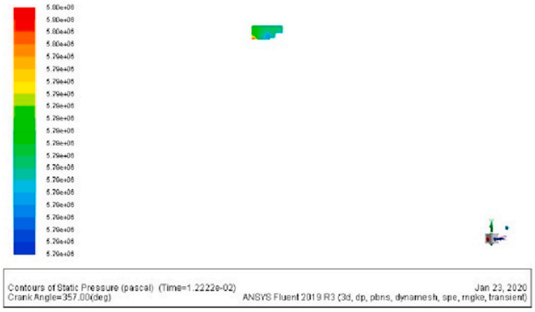

Fig. 6. B_{100} in-cylinder CFD combustion pressure contour.

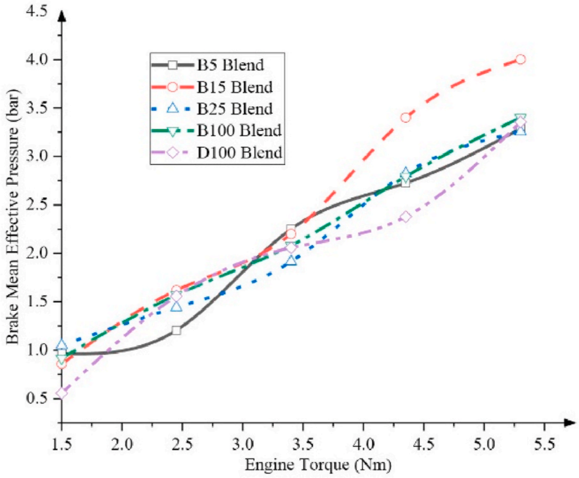

Fig. 7. Experimental combustion in-cylinder pressure.

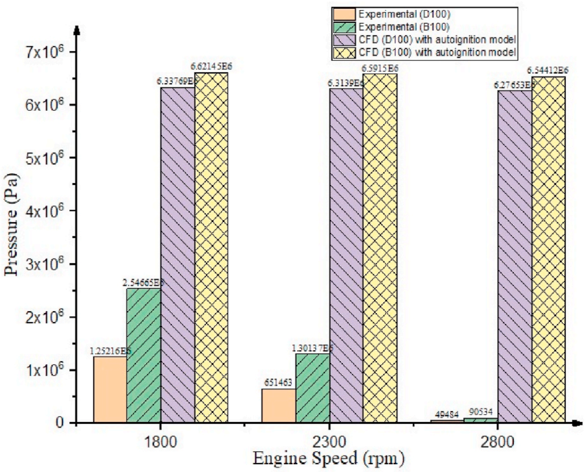

Fig. 8. Experimental and numerical combustion characteristics comparison.

mechanical energy. In this wise, all blends in Fig. 14 had a steady rise in BTE with torque, however, B_{15} and D_{100} negotiated an apparent fall from 4.35 Nm due to power or heat released negation response in each. In addition, B_{100} presented a better quasi-linear curve and B_{25} made the highest conversion response. Kader et al.; Onuh and Inambao [51,52] experimented similar trend.

Table 5
Properties of Khaya senegalensis fuel blends.

Properties	Samples					ASTM		
	B_5	B_{15}	B_{25}	B_{100}	D_{100}	Method	$B_{6\text{-}20}$ (D 7467)	B_{100} (D 6751)
Density at 15 °C (kg/m^3)	862.2	863.4	864.4	874	852.8	AOAC[a]	–	–
Kinematic viscosity at 40 °C (mm^2/s)	4.763	4.655	5.005	5.862	4.635	D 445	1.9–4.1	1.9-6
Saponification value (mg KOH/g)	95.44	64.52	80.22	121.74	108.78	AOAC[a]	–	–
Iodine value (g iodine/100 g)	27.24	12.01	20.47	62.78	182.11	AOAC[a]	–	–
Cetane Number	97.36	128.19	109.73	77.01	55.5	D 613	40 min.	47 min.
Cloud point (°C)	0.2	0.4	0.7	8.3	0.2	D 2500	Report	Report
Pour point (°C)	< -1.5	< -1.5	< -1.5	2	< -1.5	D 97-96a	–	–
Smoke point (°C)	68	70	75	89.3	67	D 93	–	–
Flash point (°C)	95	97	98	124	83	D 93	125 min.	130 min.
Calorific value- LHV (MJ/kg)	39.905	39.754	39.603	37.443	35.65	AOAC[a]	–	–

[a] AOAC (Association of Official Analytical Chemists) standard method of 1995.

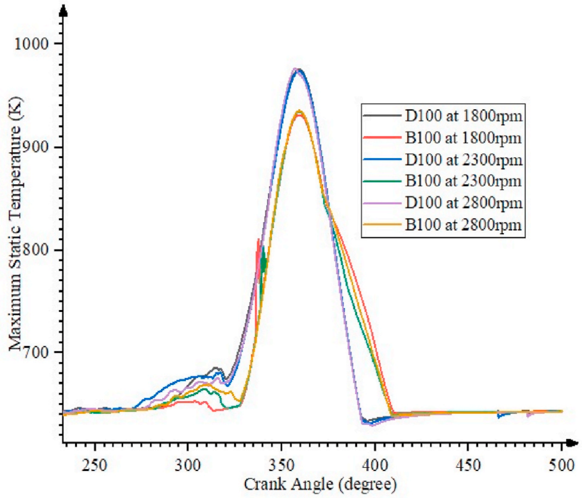

Fig. 9. CFD combustion temperature plots.

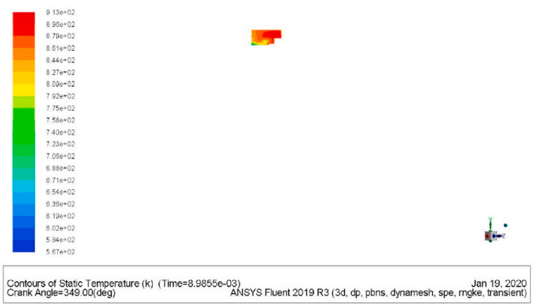

Fig. 10. In-cylinder combustion temperature of D_{100}.

4.5. Emission: CO_2

Fig. 15 profile is segmented into two phases for D_{100} emission. The first has a CO_2 highest peak value mass fraction of 4.73 exp-4 at 341.45° CA for 1800 rpm and this early combustion will exist for all three speed in 333.25°–410° CA span. The second phase will possess the massive CO_2 emission during expansion phase in mass fractions of 4.65 exp-4 at 495° CA, 5.09 exp-4 distributing through 474°–480° CA and 5.08 exp-3 at 489° CA for 1800, 2300 and 2800 rpm respectively. Emissions profile of B_{100} is predicted quantitatively more than D_{100} spreading through 335°–399° CA with maximum mass fraction of 4.81 exp-4, 4.79 exp-4 and 4.8exp-4 for the respective speeds. This may have stemmed from excessive volatile matters that promoted complete combustion in time, unlike the D_{100} that has the likelihood of emitted unburned hydrocarbon running through the expansion stroke.

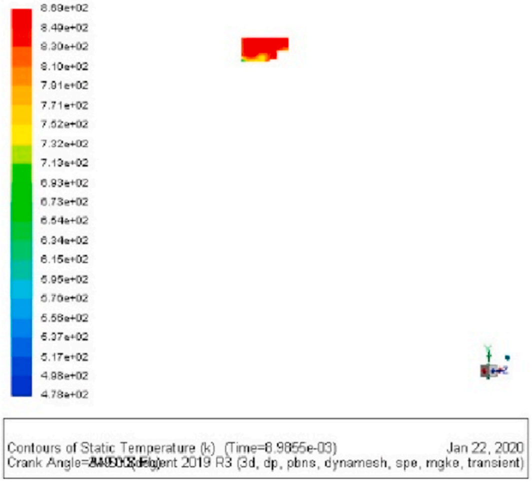

Fig. 11. In-cylinder combustion temperature of B_{100}.

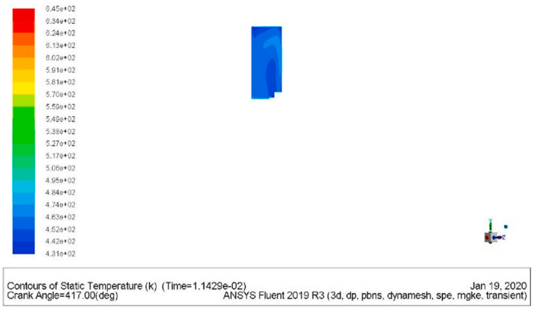

Fig. 12. Expansion stroke in-cylinder temperature of D_{100} at 417° CA.

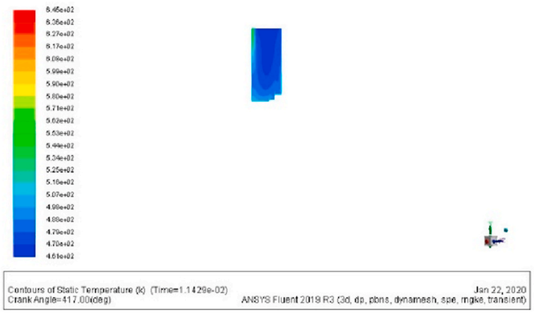

Fig. 13. Expansion stroke in-cylinder temperature of B_{100} at 417° CA.

Measurement of CO_2 experiment result in Fig. 16 presented B_5, B_{15}, B_{25}, and B_{100} emissions on increasing load to be 47.01 % (470,100 ppm), 8.07 % (80,700 ppm), 21.72 % (217,200 ppm) and 6.06 % (60,600 ppm) lower than D_{100}. Hence B_5 made the best performance on CO_2 emission.

5. Conclusions

This article attempts to concurrently improve the performance of a diesel single cylinder ICE and also reduce its CO_2 emission through a 3D model engine simulation on ANSYS fluent before an experimented combustion.

✓ From the discussion above, numerical predictions of the combustion served well and were validated quite appropriately.

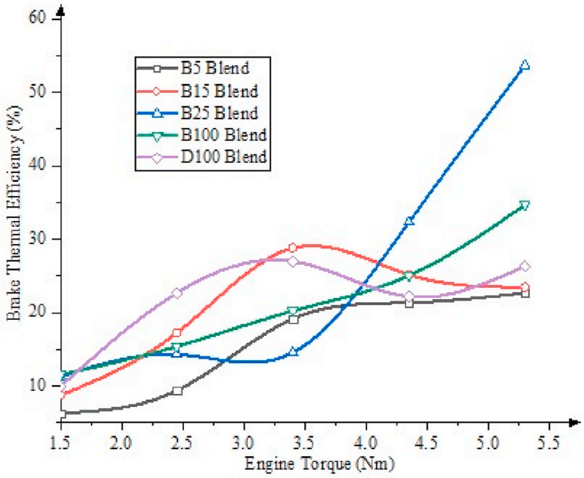

Fig. 14. Fuel blends BTE engine performance responses to loading.

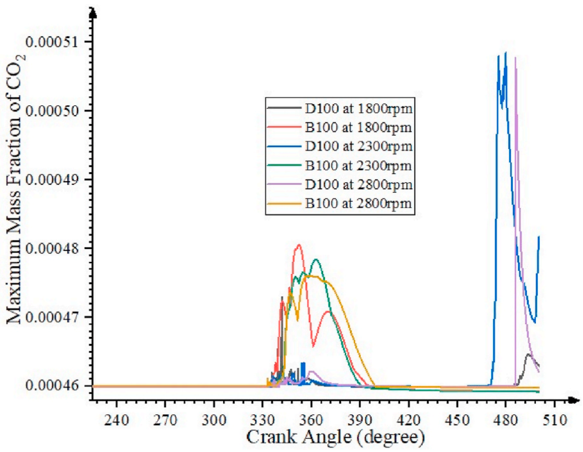

Fig. 15. Numerical prediction of CO_2 emission.

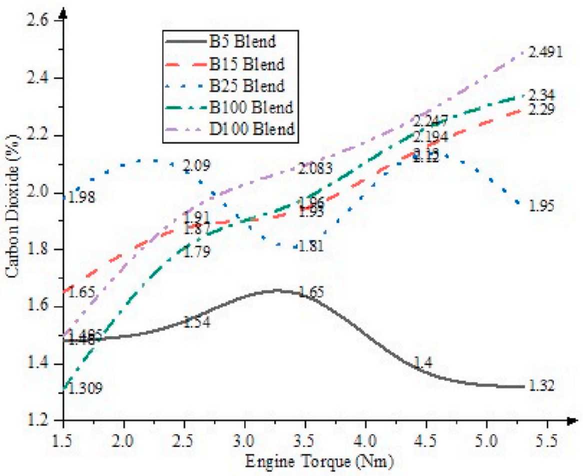

Fig. 16. Percentage mass concentration of CO_2 emission.

- ✓ Blends of B_{15} and below will maintain good performance and lower CO_2 emission than D_{100}. This will offer a good depletion on the global warming effect.
- ✓ Other emission potentials of this biodiesel substrate could be determined for wider spread conclusion.

Funding source

This study was a self-sponsored work without any funding support from individual, organization or Agency.

Data availability statement

No data was used for the research described in this article.

CRediT authorship contribution statement

Elijah Eferoghene Onojowho: Writing – review & editing, Writing – original draft, Software, Methodology, Investigation. **Eriola Betiku:** Supervision, Resources. **Abraham Awolola Asere:** Supervision, Conceptualization.

Declaration of competing interest

The authors declare the following financial interests/personal relationships which may be considered as potential competing interests:

Onojowho E. E. reports equipment, drugs, or supplies was provided by Mechanical Engineering Department, University of Benin.

Acknowledgement

Authors sincerely appreciate the Department of Mechanical Engineering, University of Benin for granting access to their equipment's and laboratory.

Nomenclature

BMEP	Brake mean effective pressure (bar)
TDC	Top dead center
BTE	Brake thermal efficiency (%)
ICEM	Internal Combustion Engine Modeler
LHV	Lower heating value (MJ/kg)
ICE	Internal combustion engine
CI	Compression ignition
B_5 5%	biodiesel, 95% diesel blend
B_{15}	15% biodiesel, 85% diesel blend
B_{25}	25% biodiesel, 75% diesel blend
B_{100}	Pure biodiesel
D_{100}	Pure diesel
ANSYS	Analysis of System
BNEF	BloombergNEF
CFD	Computational fluid dynamics
BSFC	Brake specific fuel consumption (Kg.kW/h)
CO_2	Carbon (iv) oxide
BDC	Bottom dead center
ABDC	After bottom dead center
BBDC	Before bottom dead center
SI	Spark ignition
HCCI	Homogeneous charge compression ignition
CAI	Controlled autoignition
SCDM	SpaceClaim design modeler
CA	Crank angle
RNG	Renormalized group
ppm	Part per million
IVC	Inlet valve close

References

[1] B.R. Moser, Biodiesel production, properties, and feedstock, In Vitro Cell. Dev. Biol. Plant 45 (2009) 229–266, https://doi.org/10.1007/s11627-009-9204-z.

[2] IRENA, Advanced biofuels. What holds them back? Int. Renew. Energy Agency (2019). Abu Dhabi, www.irena.org/publications.

[3] B. John, J. Freel, A. Gibbs, L. Gibbs, G. Hemighaus, k Hoekman, H. Jerry, G. Andy, I. Michael, Andrea Tiedemann, Chuck Walker, John Lind, Jacqueline Jones, Deborah Scott, Jennifer Mills, Diesel Fuels Technical Review., Chevron, Chevron Products Company 6001 Bollinger Canyon Road San Ramon, CA 94583, 2007. www.chevron.com/products/prodserv/fuels/bulletin/diesel.

[4] T.N. Verma, P. Shrivastava, U. Rajak, G. Dwivedi, S. Jain, A. Zare, A.K. Shukla, P. Verma, A comprehensive review of the influence of physicochemical properties of biodiesel on combustion characteristics, engine performance and emissions, J. Traffic Transport. Eng. 8 (2021) 510–533, https://doi.org/10.1016/j.jtte.2021.04.006.

[5] J.J. Cheng, G.R. Timilsina, Status and barriers of advanced biofuel technologies: a review, Renew. Energy 36 (2011) 3541–3549, https://doi.org/10.1016/j.renene.2011.04.031.

[6] P. Lyu, P. Slade Wang, Y. Liu, Y. Wang, Review of the studies on emission evaluation approaches for operating vehicles, J. Traffic Transport. Eng. 8 (2021) 493–509, https://doi.org/10.1016/j.jtte.2021.07.004.

[7] C. Panoutsou, S. Germer, P. Karka, S. Papadokostantakis, Y. Kroyan, M. Wojcieszyk, K. Maniatis, P. Marchand, I. Landalv, Advanced biofuels to decarbonise European transport by 2030: markets, challenges, and policies that impact their successful market uptake, Energy Strategy Rev. 34 (2021) 1–23, https://doi.org/10.1016/j.esr.2021.100633.

[8] Y. Yang, Z. Tian, Y. Lan, S. Wang, H. Chen, An overview of biofuel power generation on policies and finance environment, applied biofuels, device and performance, J. Traffic Transport. Eng. 8 (2021) 534–553, https://doi.org/10.1016/j.jtte.2021.07.002.

[9] M.N.A.M. Yusoff, N.W.M. Zulkifli, N.L. Sukiman, O.H. Chyuan, M.H. Hassan, M.H. Hasnul, M.S.A. Zulkifli, M.M. Abbas, M.Z. Zakaria, Sustainability of palm biodiesel in transportation: a review on biofuel standard, policy and international collaboration between Malaysia and Colombia, Bioenerg. Res. 14 (2021) 43–60, https://doi.org/10.1007/s12155-020-10165-0.

[10] A.P. Atta, A. Diango, Y. N'Guessan, G. Descombes, C. Morin, A. Jaecker-Voirol, Life cycle assessment, technical and economical analyses of jatropha biodiesel for electricity generation in remote areas of côte d'Ivoire, in: Refining Biomass Residues for Sustainable Energy and Bioproducts, Elsevier, 2020, pp. 523–542, https://doi.org/10.1016/B978-0-12-818996-2.00024-7.

[11] J. Xue, T.E. Grift, A.C. Hansen, Effect of biodiesel on engine performances and emissions, Renew. Sustain. Energy Rev. 15 (2011) 1098–1116, https://doi.org/10.1016/j.rser.2010.11.016.

[12] A.B. Delshad, L. Raymond, V. Sawicki, D.T. Wegener, Public attitudes toward political and technological options for biofuels, Energy Pol. 38 (2010) 3414–3425, https://doi.org/10.1016/j.enpol.2010.02.015.

[13] Y.-K. Oh, K.-R. Hwang, C. Kim, J.R. Kim, J.-S. Lee, Recent developments and key barriers to advanced biofuels: a short review, Bioresour. Technol. 257 (2018) 320–333, https://doi.org/10.1016/j.biortech.2018.02.089.

[14] E. Christensen, R.L. McCormick, Long-term storage stability of biodiesel and biodiesel blends, Fuel Process. Technol. 128 (2014) 339–348, https://doi.org/10.1016/j.fuproc.2014.07.045.

[15] S. Ramkumar, V. Kirubakaran, Biodiesel from vegetable oil as alternate fuel for C.I engine and feasibility study of thermal cracking, Energy Convers. Manag. 118 (2016) 155–169, https://doi.org/10.1016/j.enconman.2016.03.071.

[16] Y. Zhang, Y. Zhong, S. Lu, Z. Zhang, D. Tan, A comprehensive review of the properties, performance, combustion, and emissions of the diesel engine fueled with different generations of biodiesel, Processes 10 (2022) 1–55, https://doi.org/10.3390/pr10061178.

[17] BNEF, E-buses to surge even faster than EVs as conventional vehicles fade, 2018. https://about.bnef.com/blog/e-buses-surge-even-faster-evs-conventional-vehicles-fade/ (accessed October 14, 2019).

[18] P. Barua, N. Hossain, T. Chowdhury, H. Chowdhury, Commercial diesel application scenario and potential of alternative biodiesel from waste chicken skin in Bangladesh, Environ. Technol. Innov. 20 (2020) 101139, https://doi.org/10.1016/j.eti.2020.101139.

[19] J. Shi, Y. Zhu, Y. Feng, J. Yang, C. Xia, A prompt decarbonization pathway for shipping: green hydrogen, ammonia, and methanol production and utilization in marine engines, Atmosphere 14 (2023) 1–29, https://doi.org/10.3390/atmos14030584.

[20] D. Tan, Y. Meng, J. Tian, C. Zhang, Z. Zhang, G. Yang, S. Cui, J. Hu, Z. Zhao, Utilization of renewable and sustainable diesel/methanol/n-butanol (DMB) blends for reducing the engine emissions in a diesel engine with different pre-injection strategies, Energy 269 (2023) 1–19, https://doi.org/10.1016/j.energy.2023.126785.

[21] H. Bakir, U. Agbulut, A.E. Gurel, G. Yildiz, U. Guvenc, M.E.M. Soudagar, A.T. Hoang, B. Deepanraj, G. Saini, A. Afzal, Forecast of future greenhouse gas emission trajectory for India using energy and economic indexes with various metaheuristic algorithms, J. Clean. Prod. 360 (2022) 131946, 10.1016/j.jclepro.2022.131946.

[22] D. Tan, Y. Wu, J. Lv, J. Li, X. Ou, Y. Meng, G. Lan, Y. Chen, Z. Zhang, Performance optimization of a diesel engine fueled with hydrogen/biodiesel with water addition based on the response surface methodology, Energy 263 (2023) 125869, https://doi.org/10.1016/j.energy.2022.125869.

[23] A.A. Yusuf, J.D. Ampah, M.E.M. Soudagar, I. Veza, U. Kingsley, S. Afrane, C. Jin, H. Liu, A. Elfasakhany, K. Buyondo, Effects of hybrid nanoparticle additives in n-butanol/waste plastic oil/diesel blends on combustion, particulate and gaseous emission from diesel engine evaluated with entropy-weighted PROMETHEE II and TOPSIS: environmental and health risks of plastic waste, Energy Convers. Manag. 264 (2022) 115758, 10.1016/j.enconman.2022.115758.

[24] M.E.M. Soudagar, A. Afzal, R.M. Safaei, M.A. Manokar, A.I. EL-Seesy, M.A. Mujtaba, O.D. Samuel, I.A. Badruddin, W. Ahmed, K. Shahapurkar, M. Goodarzi, Investigation on the effect of cottonseed oil blended with different percentages of octanol and suspended MWCNT nanoparticles on diesel engine characteristics, J. Therm. Anal. Calorim. 1 (2020) 1–18, 10.1007/s10973-020-10293-x.

[25] M.E.M. Soudagar, N.-N. Nik-Ghazali, M.A. Kalam, I.A. Badruddin, N.R. Banapurmath, Y.T.M. Khan, N.M. Bashir, N. Akram, R. Farade, The effects of graphene oxide nanoparticle additive stably dispersed in dairy scum oil biodiesel-diesel fuel blend on CI engine: performance, emission and combustion characteristics, Fuel 257 (2019) 1–17, 10.1016/j.fuel.2019.116015.

[26] M.E.M. Soudagar, M.A. Mujtaba, R.M. Safaei, A. Afzal, V. Dhana Raju, W. Ahmed, N.R. Banapurmath, N. Hossain, S. Bashir, I.A. Badruddin, M. Goodarzi, K. Shahapurkar, N.S. Taqui, Effect of Sr@ZnO nanoparticles and Ricinus communis biodiesel-diesel fuel blends on modified CRDI diesel engine characteristics, Energy 215 (2021) 119094, 10.1016/j.energy.2020.119094.

[27] H. Venu, V. Dhana Raju, S. Lingesan, M.E.M. Soudagar, Influence of Al2O3nano additives in ternary fuel (diesel-biodiesel-ethanol) blends operated in a single cylinder diesel engine: performance, Combustion and Emission Characteristics, Energy 20 (2020) 1–65, https://doi.org/10.1016/j.energy.2020.119091.

[28] Z. Zhang, J. Ye, D. Tan, Z. Feng, J. Luo, Y. Tan, Y. Huang, The effects of Fe2O3 based DOC and SCR catalyst on the combustion and emission characteristics of a diesel engine fueled with biodiesel, Fuel 290 (2021) 1–11, https://doi.org/10.1016/j.fuel.2020.120039.

[29] L. Razzaq, M.A. Mujtaba, M. Soudagar Manzoore Elahi, W. Ahmed, H. Fayaz, S. Bashir, I.M.R. Fattah, H. Chyuan Ong, K. Shahapurkar, A. Afzal, S. Wageh, A. Al-Ghamdi, M.S. Ali, A.I. EL-Seesy, Engine performance and emission characteristics of palm biodiesel blends with graphene oxide nanoplatelets and dimethyl carbonate additives, J. Environ. Manag. 282 (2021) 1–10, https://doi.org/10.1016/j.jenvman.2020.111917.

[30] M. Barot, A. Shah, M. Patel, CFD analysis of single cylinder four stroke gas fueled engine for prediction of air flow rate during suction stroke, IJEDR 5 (2017) 1135–1140.

[31] M. Aghbashlo, W. Peng, M. Tabatabaei, S.A. Kalogirou, S. Soltanian, H. Hosseinzadeh-Bandbafha, O. Mahian, S.S. Lam, Machine learning Technology in biodiesel research: a review, PECS 85 (2021) 1–112, https://doi.org/10.1016/j.pecs.2021.100904.

[32] M. Costa, D. Piazzullo, Biofuel powering of internal combustion engines: production routes, effect on performance and CFD modeling of combustion, Front. Mech. Eng. 4 (2018) 1–14, https://doi.org/10.3389/fmech.2018.00009.

[33] Z. Zhang, J. Li, J. Tian, R. Dong, Z. Zou, S. Gao, D. Tan, Performance, combustion and emission characteristics investigations on a diesel engine fueled with diesel/ethanol/n-butanol blends, Energy 249 (2022) 123733, https://doi.org/10.1016/j.energy.2022.123733.

[34] D.S. Gaikwad, A.V. Kolhe, Experimental validation of combustion with CFD modeling in single cylinder four stroke CI engine fueled with biodiesel, JMEST 1 (2014). www.jmest.org.
[35] A.V. Kolhe, R.E. Shelke, S.S. Khandare, Combustion modeling with CFD in direct injection CI engine fuelled with biodiesel, JJMIE 9 (2015) 61–66.
[36] S.B. Akintunde, S.O. Obayopo, A.S. Adekunle, O.R. Obisesan, O.S. Olaoye, Combustion and emission study of sandbox seed oil biodiesel performance in a compression ignition (CI) engine, Energy Rep. 7 (2021) 3869–3876, https://doi.org/10.1016/j.egyr.2021.06.070.
[37] E. Buyukkaya, Effects of biodiesel on a DI diesel engine performance, emission and combustion characteristics, Fuel 10 (2010) 3099–3105, https://doi.org/10.1016/j.fuel.2010.05.034.
[38] O. Özener, L. Yüksek, A.T. Ergenç, M. Özkan, Effects of soybean biodiesel on a DI diesel engine performance, emission and combustion characteristics, Fuel 115 (2012) 875–883, https://doi.org/10.1016/j.fuel.2012.10.081.
[39] H. Raheman, P.C. Jena, S.S. Jadav, Performance of a diesel engine with blends of biodiesel (from a mixture of oils) and high-speed diesel, Int. J. Energy Environ. Eng. 4 (2013) 1–9, 10.1186/2251-6832-4-6.
[40] M.E.M. Soudagar, N.R. Banapurmath, A. Afzal, N. Hossain, M.M. Abbas, M.A.C. Mhd Haniffa, B. Naik, W. Ahmed, S. Nizamuddin, N.M. Mubarak, Study of diesel engine characteristics by adding nanosized zinc oxide and diethyl ether additives in Mahua biodiesel-diesel fuel blend, Sci. Rep. 10 (2020) 15326, 10.1038/s41598-020-72150-z.
[41] C.-H. Yang, H. Zhao, In-cylinder studies of hybrid combustion in a direct injection single-cylinder optical engine, Int. J. Engine Res. 11 (2010) 515–531, https://doi.org/10.1243/14680874JER519.
[42] I. Veza, A. Afzal, M.A. Mujtaba, A.T. Hoang, D. Balasubramanian, M. Sekar, I.M.R. Fattah, M.E.M. Soudagar, A.I. EL-Seesy, D.W. Djamari, A.L. Hananto, N. R. Putra, N. Tamaldin, Review of artificial neural networks for gasoline, diesel and homogeneous charge compression ignition engine, Alex. Eng. J. 61 (2022) 8363–8391, 10.1016/j.aej.2022.01.072.
[43] Semin, A.R. Ismail, T.F. Nugroho, Experimental and computational of engine cylinder pressure investigation on the port injection dedicated CNG engine development, J. Appl. Sci. 10 (2010) 107–115.
[44] T. Suthisripok, P. Semsamran, The impact of biodiesel B100 on a small agricultural diesel engine, Tribol. Int. 128 (2018) 397–409, https://doi.org/10.1016/j.triboint.2018.07.042.
[45] E. Grobbelaar, The Development of a Small Diesel Engine Test Bench Employing an Electric Dynamometer, Master of Engineering, Stellenbosch University, 2017. https://scholar.sun.ac.za.
[46] E.E. Onojowho, S.O. Obayopo, A.A. Asere, Optimization of biodiesel production from Khaya senegalensis oil using heterogeneous catalyst, in: Diversification of Developing Economies: Imperatives for Sustainable Environment & Technological Innovations, OAU Printing Press, African Centre of Excellence, Obafemi Awolowo University, Ile-Ife, 2019, p. 388. www.oautekconf.org.
[47] R.S. Figliola, D.E. Beasley, Theory and Design for Mechanical Measurements, fifth ed., John Wiley & Sons, Inc, United States of America, 2011.
[48] W.M. Adaileh, K.S. Alqdah, Performance of diesel engine fuelled by a biodiesel extracted from a waste cooking oil, Energy Proc. 18 (2012) 1317–1334, https://doi.org/10.1016/j.egypro.2012.05.149.
[49] C. Ofori-Boateng, K.T. Lee, The potential of using cocoa pod husks as green solid base catalysts for the transesterification of soybean oil into biodiesel: effects of biodiesel on engine performance, Chem. Eng. J. 220 (2013) 395–401, https://doi.org/10.1016/j.cej.2013.01.046.
[50] R. Govindan, O. Jakhar, Y. Mathurv, Computational analysis of thumba biodiesel-diesel blends combustion in CI engine using ansys- fluent, Int. J. Commun. Media Stud. (IJCMS) 8 (2014) 29–39.
[51] F. Kader, A. Noor-e- Mostofa, M. Shuvo, Study of I.C. engine performance using different fuels, Interlink Continental, J. Eng. Tech. Innov. 1 (2015) 1–8.
[52] E.I. Onuh, F. Inambao, Performance and emission evaluation of pure biodiesel from non-edible feedstock and waste oil in a diesel engine, Afr. J. Sci., Technol., Innov. Dev. xx (2016) 1–12, https://doi.org/10.1080/20421338.2016.1219483.